SMAR 2019 – Fifth Conference on Smart Monitoring,
Assessment and Rehabilitation of Civil Structures

SMAR 2019

Development of Numerical Models for Deep Beams with Discontinuity Regions Strengthened by NSM-CFRP

Moustafa MANSOUR [1], Tamer EL MAADDAWY [1]
[1] UAE University, Al Ain, United Arab Emirates

Contact e-mail: tamer.maaddawy@uaeu.ac.ae

ABSTRACT: Numerical finite element (FE) models were developed to predict the load carrying capacity of three reinforced concrete (RC) deep beams. One beam was solid and two beams contained discontinuity regions in the form of a square opening located in the middle of the shear span. One of the beams with discontinuity regions was strengthened with near-surface-mounted carbon fiber-reinforced polymer (NSM-CFRP) composites. The strut-and-tie modeling (STM) procedure was employed to develop a strengthening scheme around regions of discontinuity. Several parameters were investigated during the development of the numerical model including the mesh size, concrete material constitutive law, and inclusion of a bond-slip law for the NSM-CFRP reinforcement. Numerical predictions were very sensitive to the mesh size and concrete material constitutive law adopted in the analysis. Strength results of FE models with and without a bond-slip law at the interface between the concrete and NSM-CFRP reinforcement were insignificantly different. The strengthening scheme fully restored the original shear capacity of the beam. The accuracy of the developed FE models was examined by comparing numerical predictions with those obtained from experimental tests.

1 INTRODUCTION

Transverse web openings are unavoidable in many cases because they are typically needed to provide accessibility and/or to accommodate essential services such as ventilating and air conditioning ducts. The presence of openings in RC deep beams results in an extreme geometrical discontinuity that interrupts the natural load path. Regions of extreme discontinuities in structural concrete are characterized by a complex flow of internal stresses.
Post-installed near-surface-mounted (NSM) composite reinforcement offers opportunities to prevent the FRP de bonding mode of failure as compared to externally bonded (EB) composite reinforcement (Barros and Dias 2006). The use of NSM-FRP rods on side surfaces around the openings in RC deep beams fully restored the original load capacity Pimanmas (2010).

Numerical FE modeling is a powerful approach to simulate the nonlinear behavior of complex structural elements. Hawileh et al. (2012) developed FE models to simulate the behavior of concrete beams with openings strengthened by EB-CFRP sheets. Predictions of the numerical models were compared with results of experimental tests carried out by El-Maaddawy and Sherif (2009). Good agreement between numerical and experimental results was reported. Further studies are needed to fully understand the factors affecting numerical strength predictions of RC deep beams with openings.

This paper reports the development of numerical models capable of predicting the strength of RC deep beams strengthened by NSM-CFRP around regions of discontinuities in shear spans. The numerical models were developed using the software package ATENA. The objective was

to carry out a sensitivity analysis to investigate the effect of varying key parameters on the predicted strength. The accuracy of the developed models was examined by comparing their predictions with results of experimental testing.

2 MODELS DETAILS

The current study included development of FE models for three RC deep beam specimens tested experimentally. One specimen was solid (D-S) and two specimens had discontinuity regions of a 100 x 100 mm square opening located at the middle of the shear span. The opening fully interrupted the natural load path. One of the specimens (D-O) was not strengthened whereas the third one (D-FRP) was strengthened around regions of discontinuity using inclined NSM-CFRP composite reinforcement. The beams were 2700 mm long, 500 mm deep and 150 mm wide. All beams had a shear span-to-depth ratio of a/h = 0.8. Four bars of No.16 deformed steel bars were used as main longitudinal reinforcement placed at 50 mm above the bottom surface of the beam with a side clear concrete cover of 30 mm. No internal shear reinforcement was provided in all specimens. The STM procedure was employed to develop the strengthening scheme along with the amount and distribution of CFRP reinforcement around regions of discontinuity in one of the tested specimens. Figure 1a and 1b show the layout of the developed STM and the NSM-CFRP strengthening scheme, respectively.

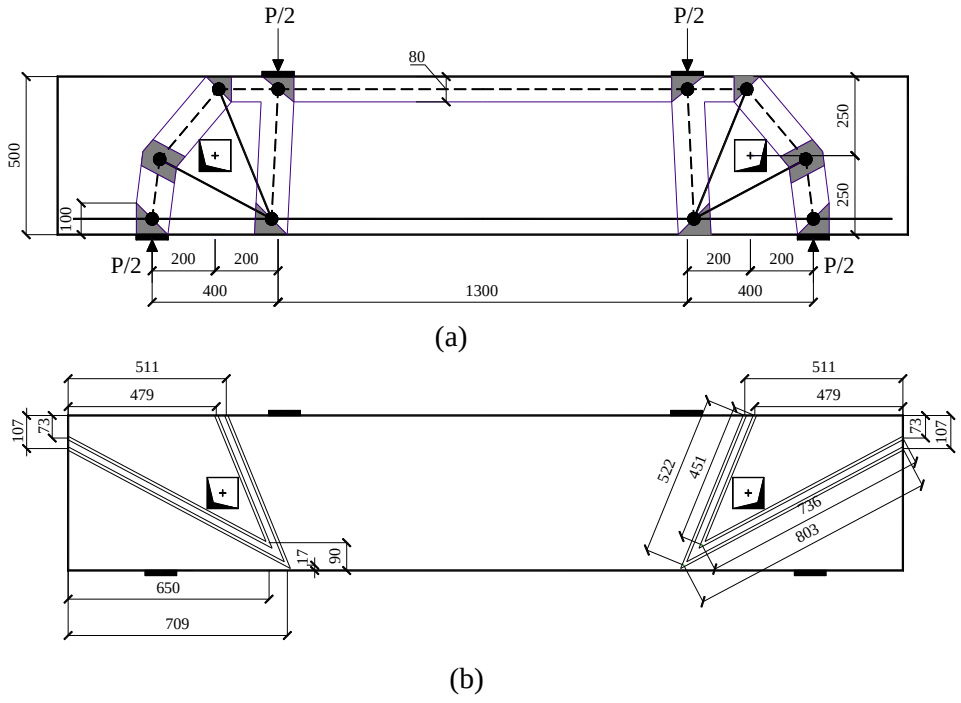

Figure 1. Specimens' details; (a) schematic of the STM, (b) NSM-CFRP strengthening layout.

Dashed lines in Figure 1a represent the centerline of struts and solid lines represent the centerline of the ties, while the shaded areas represent the nodes. The cross-sectional area of struts and nodes are calculated based on the width of the beam and the width of each member measured from the schematic drawing of the STM. Whereas the area of the ties was calculated based on the total cross-sectional area of the provided reinforcement at each tie location. The truss in the shear span included three ties, one longitudinal tie at the bottom and two inclined ties around the discontinuity region; one tie in the top chord above the opening and one tie in the bottom chord below the opening. The tie in the bottom chord was inclined at an angle of 28°

whereas the tie in the top chord was inclined at an angle of 68° with respect to the horizontal axis. The NSM-CFRP composite reinforcement were installed around the discontinuity regions based on the location and orientation of the inclined ties in STM. The CFRP plates used in strengthening had a cross section of 2.5 × 15 mm. They installed into grooves, 10 mm wide and 24 mm deep, precut on the concrete surface as shown in Figure 1b.

The nominal capacity of each member of the truss in the STM was determined as per the ACI 318-14 provisions. For a given load, the internal forces in the truss members were calculated by truss analysis. Several iterations were carried out to determine the load capacity of the truss. Preliminary calculations showed that providing two CFRP strip in each tie around the discontinuity region would cause rupture in the CFRP reinforcement. Accordingly, four CFRP strips (two strips in each side) were used in each tie around the discontinuity region to compensate the reduction in the load capacity caused by the creation of the opening. The calculated nominal load capacity of the STM was 636 kN. The load capacity was governed by failure of strut located along the inner boundary of the shear span. No failure occurred at the nodal zones.

3 MATERIALS PROPERTIES

The cube and cylinder compressive strengths of the concrete was 48 MPa and 40 MPa, respectively. The tensile splitting strength of the concrete was 3.3 MPa. The steel yield strength was 544 MPa. The tensile strength of the CFRP plates was 3100 MPa whereas their modulus of elasticity was 165 GPa. The epoxy adhesive used to bond the CFRP plates to the sides of the grooves had a tensile modulus of 4.5 GPa, tensile strength of 25 MPa, and an ultimate elongation of 1% (data were obtained from the manufacturer).

4 FE MODELING

The specimens were analyzed numerically by three-dimensional (3D) FE models using *ATENA* version 5.4. A quarter of the beam was modeled as there were two plans of symmetries in the beam geometry. Modeling a quarter of the beam made the software capable of employing a small mesh size and reduced the running time.

4.1 Mesh Sensitivity Analysis

In user's manual of ATENA, it is recommended to have a minimum of 4 to 6 elements per thickness of the beam. This corresponded to a mesh size in the range of 37.5 to 25 mm for the deep beams of the current study. A mesh sensitivity analysis was carried out to determine the optimal mesh size. In fact, as the finite elements become smaller, the software computational time increases. As a first trail, FE models were developed using a mesh size of 25 and 20 mm on half beam models. A mesh size smaller than 20 mm was not achievable in the half beam models because the software did not function when mesh size was 15 mm. To run the FE models with 15 mm mesh size, a quarter beam models were developed. Quarter beam models were run using 25, 20, and 15 mm mesh sizes.

4.2 Material Constitutive Models

The mechanical properties of concrete and reinforcements were used as input data for defining the behavior of each material. The software provides built-in material constitutive models which require few inputs from the user. In addition, it provides alternative models where the user has space to manually adjust material constitutive models. Two materials constitutive models for the concrete were studied in this research. The first model was a predefined model in the software.

The model name as in the software is "CC3DNonLinCementitious2" which is designated in this paper as DEFAULT model. The model considers concrete behavior under compression (plastic) and tension (fracturing). The details of laws and functions of the model were reported by Alkhalil and El-Maaddawy (2017).

The second used material constitutive model for concrete was named in the software as "CC3DNonLinCementitious2User". It is designated in this study as USER model. The constitutive laws in tension and compression of the USER model are almost similar to those of the DEFAULT model until the peak stress is reached at a strain value of ε_{loc}, after which the strain is localized to the finite element. The post-peak localized strain is affected by the L/L_{ch} ratio, where L = crushing band size for the compression behavior or crack band size for the tension behavior and L_{ch} = characteristic length having a default value generated by the software of 0.1 for the compression behavior and 0.03 for the tenstion behavior. The software manual recommends the value of the characteristic length, L_{ch}, for the tension behavior to be taken as that of the mesh size. The value of ε_{loc} is generated automatically by the software as function of the cube concrete strength. For the given cube strength of the concrete used in the current study (48 MPa), the value of ε_{loc} in tension was almost equal to zero, while in compression it was equal to 0.00112. Figure 2a and 2b show the compressive behavior and the tensile softening relationships, respectively, as generated by the software for the given cube concrete strength adopted in the current study.

The USER model considers a reduction in strength for cracked concrete. It assigns a reduction factor for the compressive strength, r_c, and a reduction factor for the shear strength, f_{sh}. The compressive strength reduction factor is affected by the fracturing strain (ε_f) calculated from the strain tensor at the finite element integration points whereas the shear strength reduction factor is affected by the fracturing strain after localization ($\tilde{\varepsilon}_f$) determined by Eq. 2. Figure 3a and 3b show the change in the shear and compressive strength reduction factors as per multilinear functions generated by the software.

$$\tilde{\varepsilon}_f = \varepsilon_{loc} + (\varepsilon_f - \varepsilon_{loc}) \, {}^{L}/_{L_{ch}} \tag{2}$$

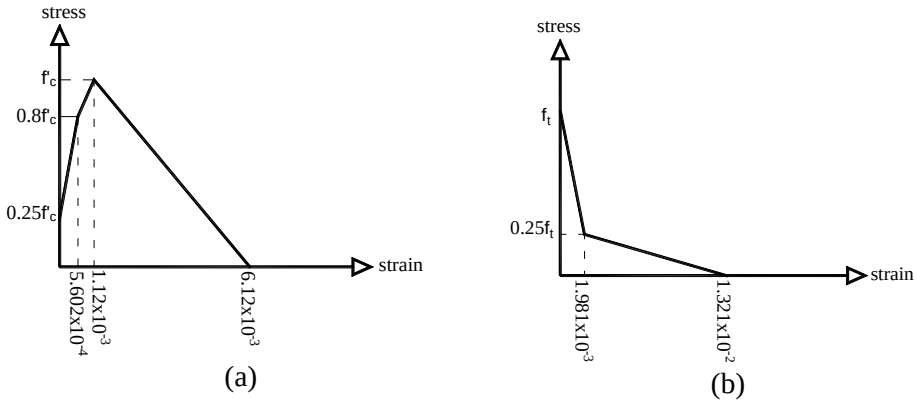

Figure 2. USER concrete material model; (a) compressive behavior, (b) tensile softening.

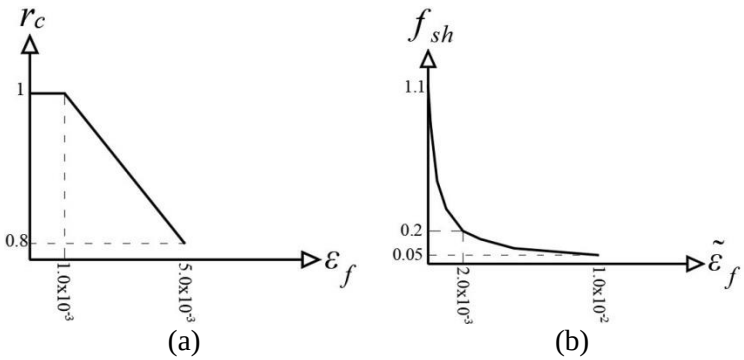

Figure 3. Functions of reduction factors for; (a) compressive strength (b) shear strength.

For both material constitutive models (DEFAULT and USER), the software requires the user to only enter the cube compressive strength of concrete. The rest of the concrete characteristics are autogenerated by built-in equations. Two properties were manually modified in both constitutive models; cylinder compressive strength which was entered as the experimental value (40 MPa) and the tensile strength which was taken as half of experimental splitting tensile strength (1.7 MPa) (Nilson et al. 2010).

The material constitutive models for reinforcements were defined by identifying the type of stress-strain curve. For reinforcement steel, the stress-strain relation was defined bilinear. The curve begins inclined linear portion with slope equal to Young's modulus of steel (E). The stress keeps increasing until yielding stress is reached. Then the stress is assumed to remain constant and equal to the tensile yield strength (f_y) as the strain keep increasing. E was 200 GPa and f_y was 544 MPa as per experimental values. The stress-strain relationship of CFRP was defined as a linear elastic curve with elastic modulus of 165 GPa. Linear-elastic behavior was also assigned to the steel plates at the support and loading points.

4.3 Bond-Slip Model

The bond between the reinforcement steel and concrete was assumed as a perfect connection. To evaluate the effect of inclusion of a bond-slip model between the CFRP and the concrete on numerical results, two models were developed for the strengthened specimen. In one model, a perfect bond was assumed between the CFRP and the concrete whereas in the other model an interfacial bond-slip model was adopted between the CFRP and the concrete. The bond-slip model developed by Ceroni et al. (2012) for the same types of CFRP plates and bonding adhesive used in the current study was adopted in the analysis. The used bond-slip model is shown in Figure 4.

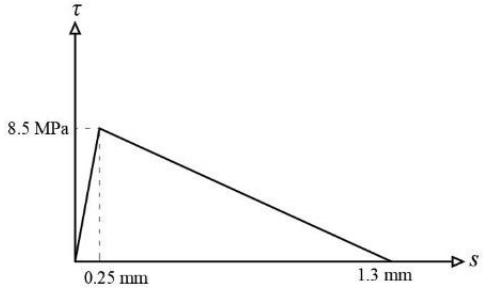

Figure 4. NSM-CFRP bond-slip model (Ceroni et al. 2012).

5 RESULTS AND DISCUSSION

Table 1 reports the mesh sensitivity analysis for the numerical models. The FE model of each specimen was run at three mesh sizes; 25 mm, 20 mm and 15 mm. The concrete material law for these models was the DEFAULT model. In addition, the NSM-CFRP reinforcement in D-FRP specimen was set to have a perfect bond with the concrete. The predictions of numerical models were compared with experimental results. The mentioned ratios in the table were calculated by dividing the predicted load capacity of each run over the corresponding experimental load capacity. It can be seen that the predicted load capacity decreased as the mesh size decreased. Predictions of all FE models with the DEFAULT concrete constitutive law were higher than the strength values obtained from experimental testing. Although predictions of the models with the smaller mesh size of 15 mm were closer to the values recorded experimentally, the predicted strengths were still 18 to 30% higher than those measured experimentally.

The effect of varying the concrete constitutive law on the numerical predictions is illustrated in Table 2. The use of the USER concrete constitutive law rather than the DEFAULT reduced the predicted load capacity and significantly enhanced the models' accuracy. FE models having the USER concrete constitutive law provided accurate predictions for the load capacity with P_{FE}/P_{Exp} ratio in the range of 0.96 to 1.09. The incorporation of the bond-slip law between the CFRP and the concrete did not reduce the load capacity predicted numerically. The NSM-CFRP strengthening scheme fully restored the load capacity of the solid beam. This was predicted numerically and verified experimentally.

Table 1. Mesh sensitivity analysis using DEFAULT concrete material model

Specimen	Numerical Strength (kN) P_{FE}			Experimental Strength (kN) P_{Exp}	Ratio P_{FE}/P_{Exp}		
	25 mm*	20 mm*	15 mm*		25 mm*	20 mm*	15 mm*
D-S	756	732	664	565	1.34	1.30	1.18
D-O	512	464	440	338	1.51	1.37	1.30
D-FRP	732	704	696	586	1.25	1.20	1.19

*Mesh size

Table 2. Comparison between numerical predictions of different concrete material models

Specimen	Numerical P_{FE}		Experimental P_{Exp}	Ratio P_{FE}/P_{Exp}	
	DEFAULT*	USER*		DEFAULT*	USER*
D-S	664	544	565	1.18	0.96
D-O	440	332	338	1.30	0.98
D-FRP	696 (728)**	632 (636)**	586	1.19 (1.24)**	1.08 (1.09)**

* Concrete material model
** With bond-slip

6 CONCLUSIONS

- The models' predictions were very sensitive to the concrete material constitutive law adopted in the analysis. FE models with the DEFAULT concrete constitutive law overestimated the load capacity.

- FE models with the smaller finite element size offered higher accuracy as the predicated strengths became closer to the experimental results. Although the use of the smaller mesh size of 15 mm improved the accuracy of the FE models with the DEFAULT concrete constitutive law, the predicted load capacity was still 18 to 30% higher than that measured experimentally.
- The use of the USER concrete constitutive law instead of the DEFAULT law significantly improved the models' accuracy. Predictions of the FE models having the USER concrete constitutive law were insignificantly different from those obtained from the test.
- The inclusion of a bond-slip law for NSM-CFRP shear reinforcement did not reduce the predicted load capacity of the strengthened beam. As such, the assumption of a perfect bond between the CFRP and concrete is valid for numerical modeling of such cases.
- The use of the STM design methodology to determine the NSM-CFRP shear reinforcement around the discontinuity region needed to fully restore the load capacity of the solid beam was successful. This was predicted numerically and verified experimentally.

7 ACKNOWLEDGMENT

The authors would like to express their gratitude to the UAEU for financing this project under Grant No. 31N372.

8 REFERENCES

Alkhalil, J. and El-Maaddawy, T., 2017. Finite element modelling and testing of two-span concrete slab strips strengthened by externally-bonded composites and mechanical anchors. *Engineering Structures*, *147*, pp.45-61.

American Concrete Institute, 2014. *Building Code Requirements for Structural Concrete (ACI 318-14): an ACI Report*. American Concrete Institute. ACI.

ATENA [Computer software]. Červenka Consulting s.r.o., Prague, Czech Republic.

Barros, J.A. and Dias, S.J., 2006. Near surface mounted CFRP laminates for shear strengthening of concrete beams. *Cement and Concrete Composites*, *28*(3), pp.276-292.

Ceroni, F., Pecce, M., Bilotta, A. and Nigro, E., 2012. Bond behavior of FRP NSM systems in concrete elements. *Composites Part B: Engineering*, *43*(2), pp.99-109.

El Maaddawy, T. and Sherif, S., 2009. FRP composites for shear strengthening of reinforced concrete deep beams with openings. *Composite Structures*, *89*(1), pp.60-69.

Hawileh, R.A., El-Maaddawy, T.A. and Naser, M.Z., 2012. Nonlinear finite element modeling of concrete deep beams with openings strengthened with externally-bonded composites. *Materials & Design*, *42*, pp.378-387.

Nilson, A.H., Darwin, D. and Dolan, C.W., 2010. *Design of concrete structures 14th ed*. McGraw-Hill Higher Education.

Pimanmas, A., 2010. Strengthening R/C beams with opening by externally installed FRP rods: Behavior and analysis. *Composite Structures*, *92*(8), pp.1957-1976.